Stark effect in argon Rydberg states

P. F. Brevet, M. Pellarin, and J. L. Vialle
Laboratoire de Spectrométrie Ionique et Moléculaire, Université Lyon I, F-69622 Villeurbanne, France
(Received 12 March 1990)

We have applied the collinear laser spectroscopy technique to investigate the Stark structure of argon Rydberg states in the vicinity of the $n=18$ hydrogenic manifold below the first ionization limit ($3p^5\,^2P_{3/2}$ ionic core). Stark spectra have been recorded for electric fields from 0 up to 120 V/cm. Although the studied energy range is only 4 cm^{-1} wide, it is sufficient to observe how the $18f$ level progressively merges into the hydrogenic linear Stark structure arising from the $n=18$ ($l \geq 4$) manifold. The high resolution of the method allowed us to observe several fine-structure components for each Stark level. The complexity of these spectra mainly originates in the electrostatic interaction of the Rydberg electron with an anisotropic ionic core. Using jK coupling, a calculation is developed that quantitatively fits the observed spectra. The energy positions of the lines, as well as their relative intensities, are accurately reproduced by this calculation. The best fit between theory and experiment is obtained when we take into account the presence of the odd-parity perturber state $18d[3/2]_1$, which is known to lie within the studied energy range.

I. INTRODUCTION

Collinear laser spectroscopy has proved to be a very efficient method for investigating Rydberg states of rare gases, for example, Ar.[1] By simply adding a static homogeneous electric field along the interaction region, it is possible to extend this method to Stark-effect studies in rare gases. Our initial purpose was only to determine the J values of a few Ar Rydberg levels by observing their quadratic Stark structures, since, in some cases, field-free spectroscopy turned out to be insufficient to identify clearly the various fine-structure components of a Rydberg state, mainly near the $9p'$ and $10p'$ perturbers. But it rapidly appeared that systematic studies of the Stark effect in argon Rydberg states were possible with our setup, and this paper is essentially devoted to the results obtained from these studies.

The Stark effect on Rydberg levels was investigated at first in alkali-metal and alkaline-earth atoms.[2-6] This corresponds to the simplest case of a Rydberg electron interacting with an isotropic ionic core together with the external Stark field. The extension of these studies to other atoms, for example, noble gases, introduces a more complex physical situation, since the ionic core now becomes anisotropic, as pointed out by Kelleher and Saloman.[7] The increasing experimental difficulties—the laser wavelengths required, for instance—also explain why the results are much less abundant for rare gases than for alkali-metal elements. However, several papers devoted to this subject have been published during the past few years. The Stark effect of the autoionizing Rydberg states was investigated by Delsart and Keller[8] in Kr and by Ernst, Softley, and Zare[9] in Xe. The Stark structure of the bound Rydberg states of Xe, below the $^2P_{3/2}$ ionization limit, was studied by Knight and Wang.[10] In addition, we can also mention the investigation of Stark splittings and shifts of Ne lines in the visible range by Jäger and Windholz[11] and Ziegelbecker and Schnizer.[12] On the other hand, the work of Kelleher and Saloman[7] on the Stark spectra of the $5d_{3/2}8l$ autoionizing states in Ba deals with the same problem, since the excited $5d_{3/2}$ ionic core shows the same anisotropy.

In this paper, we report the results of Stark-effect measurements in the vicinity of the $n=18$ manifold of the lowest Rydberg series ($^2P_{3/2}$ core) of argon. These Rydberg levels are populated by laser excitation from the $3p^5 4s[3/2]_2$ metastable state. Since this metastable state is not perfectly pure but is weakly mixed with some levels of the $3p^5 3d$ configuration,[13] the populated Rydberg levels include the nf series in addition to the np series.[1] Due to their small quantum defects, these nf levels are very close to the hydrogenic nl ($l>3$) manifold. Several Stark maps were recorded, covering a frequency range of ± 2 cm^{-1} on both sides of the $n=18$ hydrogenic manifold and for various dc Stark fields from 0 to 120 V/cm, in order to observe how the $18f$ levels progressively merges with the linear hydrogenic Stark manifold. This study is well adapted to our experimental technique, which is characterized by a very high resolution (about 5×10^{-3} cm^{-1}) but a relatively small, continuously tunable frequency range. In other words, the Stark maps we are presenting here for argon correspond to a small part of the Stark maps obtained by Knight and Wang[10] for xenon but with a much better resolution. It is also important to note that the choice of the $4s[3/2]_2$ metastable state as starting level for the Rydberg states excitation process was imposed because of the available uv laser frequency. However, it would have been simpler, for the analysis of the Stark spectra, to start from the $4s'[1/2]_0$ metastable state as pointed out by Knight and Wang.[10]

II. EXPERIMENTAL PROCEDURE

The experimental setup has been described elsewhere in detail[1] and will only be summarized here. A fast

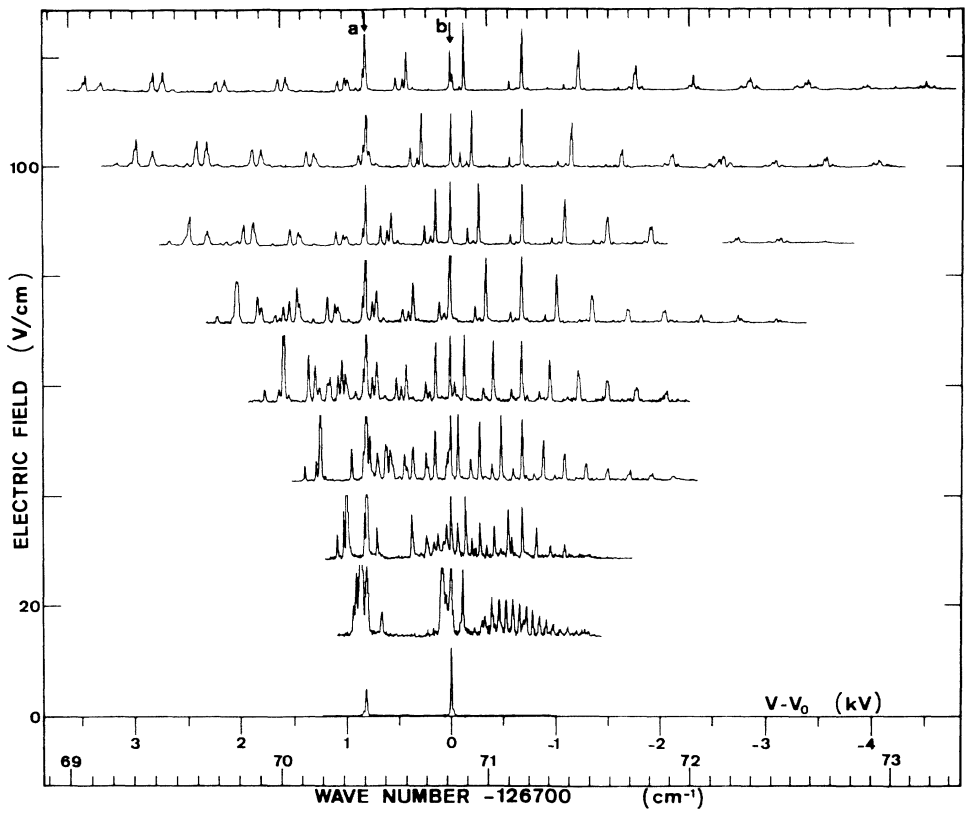

FIG. 1. Experimental Stark map for $|M|=0,1,2$ states of argon near $n=18$ (positions of zero-field lines are indicated by arrows a and b). The absolute scale for line intensities is arbitrary chosen for each electric field value. Some lines may be truncated. $V-V_0$ is the voltage offset applied on the charge-exchange cell for Doppler tuning.

monoenergetic ionic beam of argon is neutralized in flight by passing through a sodium vapor.[14] This charge exchange process efficiently populates the metastable states $4s[3/2]_2$ and $4s'[1/2]_0$ of neutral argon. Downstream from the charge-exchange cell, the neutral atoms interact collinearly with an uv laser beam. This uv radiation is produced by the intracavity frequency-doubling technique in a cw single-mode ring dye laser running with Rhodamine 6G.[15]

The uv frequency range available with our setup allows us to excite the argon atoms from the metastable state $4s[3/2]_2$ directly into the high-lying Rydberg states below the first ionization limit ($3p^5\,^2P_{3/2}$). The interaction between the laser beam and the atomic beam takes place along a common path about 1 m long. As they leave this interaction zone the Rydberg atoms are ionized by a static electric field; the produced ions are deflected and collected into a Faraday cup. As usually done in collinear spectroscopy experiments, the laser is kept at a fixed frequency and the optical resonances are scanned by Doppler tuning.[16] For this purpose a linear ramp voltage is applied to the charge-exchange cell and the ionic current is recorded as a function of this postacceleration voltage.

In order to observe the Stark effect in the Rydberg states two parallel electric plates, 40 cm long, are set in the interaction region on both sides of the atomic beam. The spacing between the plates is only (14 ± 0.1) mm and the Stark field can be continuously chosen between 0 and 1000 V/cm or even more. The atoms of the beam interact with the laser radiation successively in the presence of a constant electric field and then in a field-free region, the transition between these two situations being very sharp. Therefore we observe on the same recording the Stark structure corresponding to a given electric field as well as the field-free Rydberg levels; the latter are very convenient as frequency markers to get a common frequency scale for several recordings obtained with various Stark fields (see Fig. 1). It is also possible to rotate the field plates around the beam axis and to set the Stark electric field either parallel or perpendicular to the direction of the laser polarization allowing $\pi(\Delta M=0)$ or $\sigma(\Delta M=\pm1)$ excitations.

III. EXPERIMENTAL RESULTS

By observing the quadratic Stark effect of an isolated energy level, it is possible to determine the J value associated to this level: the number of Stark components as well as their relative intensities for both σ or π excitations are related in a well-known way to the J value and allow J to be found without ambiguity. In that way some uncertainties remaining in the level assignment obtained from field-free spectroscopy[1] are removed and the levels

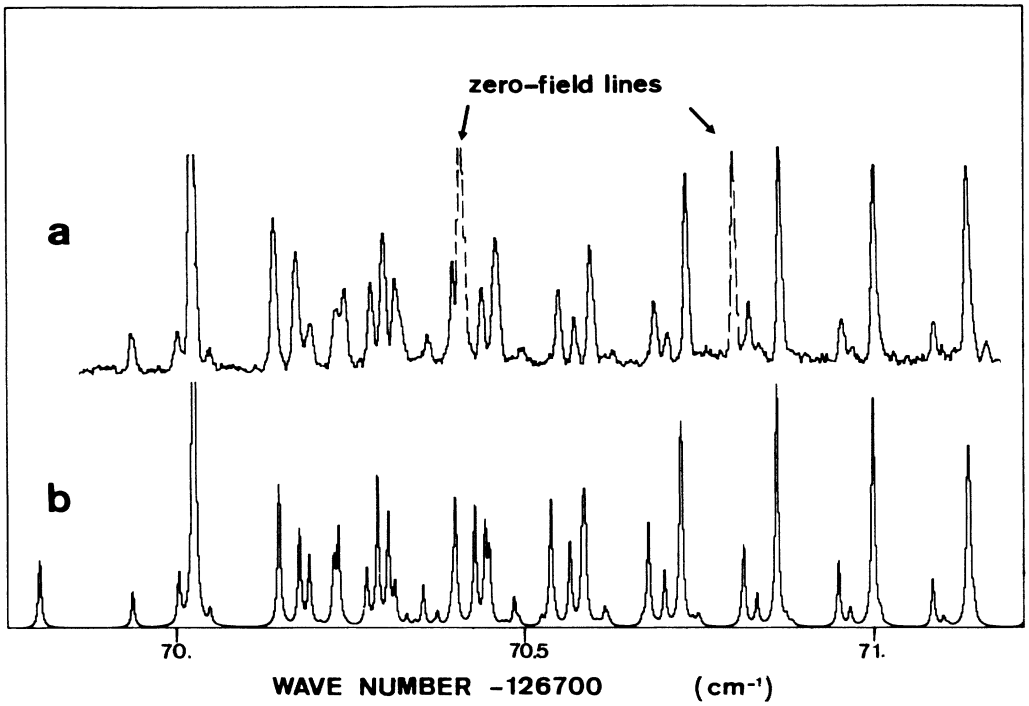

FIG. 2. Enlarged portion of the $F=58$ V/cm spectra. Curve *a*, experimental spectrum; curve *b*, theoretical spectrum.

at 126 486.36, 126 489.11, 126 955.27, and 126 956.74 cm^{-1} are clearly identified as $9p'[3/2]_1$, $15p[5/2]_2$, $10p'[1/2]_1$, and $10p'[3/2]_2$, respectively (see Table 1 in Ref. 1).

The experimental results obtained on the Stark spectra in the vicinity of the $n=18$ hydrogenic manifold are displayed in Fig. 1. Since we start from a $J=2$ level and operate with a π excitation, the Stark manifolds $|M|=0,1,2$ are simultaneously observed. The zero-field spectrum, which is described elsewhere,[1] comprises two fine-structure doublets $18f[3/2]_{2,1}$ and $18f[5/2]_{3,2}$ belonging to the $18f$ level. They are indicated on the figure by arrows *a* and *b*, respectively. As explained above, the peaks corresponding to this zero-field spectrum are present in all the spectra whatever the Stark field is. For a very low Stark field ($F<20$ V/cm) one observes the appearance of a linear Stark spectrum with equally spaced components originating from the $n=18l>3$ manifold and a quadratic Stark effect for the doublets of the $18f$ level. The isolated peak, appearing on the right-hand side of the $18f[3/2]_{2,1}$ doublet originates probably from the $18d[3/2]_1$ component of the $18d$ level, which is mixed by the Stark interaction with the $18f$ level. This sublevel was tabulated by Yoshino[17] at 126 770.5 cm^{-1} and this is the only state of opposite parity which is expected within the frequency range studied.

When the Stark field increases, the fine-structure components of the $18f$ level are progressively included in the linear Stark manifold yielding a very complicated structure on the left-hand side of the Stark spectra. For higher Stark field ($F>80$ V/cm) the Stark spectrum becomes regular again. Since the $18f$ level is completely included in the linear Stark splitting, 15 equidistant Stark components are observed, as expected ($18s$, $18p$, and $18d$ states are still absent at this electric field strength). But each Stark component presents a "fine structure" formed by several neighboring peaks. The linewidth of the experimental resonances is about 5×10^{-3} cm^{-1}. To give a better idea of the resolution and of the detailed structure, two enlargements of typical parts of the experimental Stark map shown in Fig. 1 are presented in Figs. 2(a) and 3(a).

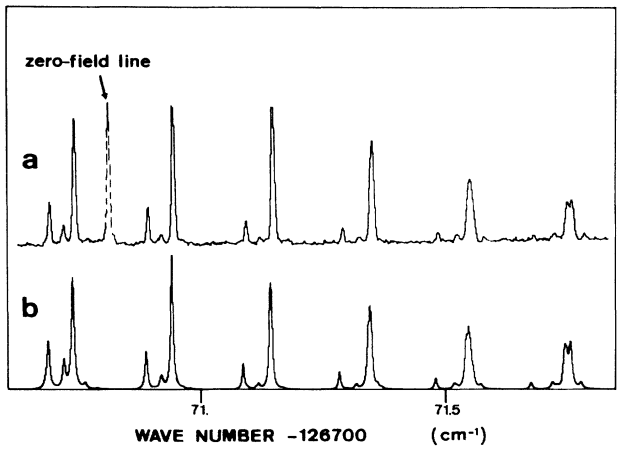

FIG. 3. Enlarged portion of the $F=86$ V/cm spectra in the vicinity of the manifold center. Curve *a*, experimental spectrum; curve *b*, theoretical spectrum.

IV. THEORETICAL TREATMENT

Owing to the relative simplicity of the physical system described in this paper, it is possible to simulate the observed spectra by performing a complete diagonalization of the total Hamiltonian $H=H_0+H_{\text{Stark}}$ in a well-suited truncated basis.[12] Such a calculation has been successfully performed by Kelleher and Saloman[7] for the almost similar case of autoionizing Rydberg states in barium. We begin by introducing the numerical procedure leading to the construction of the synthetic spectra. This section is followed by a section on the successive steps of the calculation which are described in more detail, together with the approximations required. Finally, we shall discuss the theoretical results and compare them with experimental data.

A. Calculation procedure

The different steps of the Stark spectra calculation are the following.

(i) A truncated basis set of zero-field states is chosen in the best coupling scheme and the zero-field energies are calculated assuming the atomic Hamiltonian H_0 to be diagonal in this basis.

(ii) The nondiagonal matrix elements originating from the Stark Hamiltonian $H_{\text{Stark}}=-Fz$ (a.u.) are computed for each experimental value of the electric field F.

(iii) The total Hamiltonian $H=H_0+H_{\text{Stark}}$ is diagonalized for each F and each accessible M value ($M=0,\pm1,\pm2$), M being the total magnetic quantum number, which remains the only one good quantum number of the system. Thanks to the $\pm M$ degeneracy of the atomic states in an electric field the computation is performed for positive M values only.

(iv) The energies of Stark levels are deduced from H eigenvalues, and the corresponding relative line intensities for a F spectrum are calculated using H eigenfunctions.

(v) The synthetic spectra to be compared with the experimental data are obtained by adding the three spectra corresponding to $|M|=0,1,2$ for a given F value and by performing a convolution with a line shape to reproduce the experimental Doppler broadening.

B. Discussion of the successive steps and approximations

The jK coupling scheme has revealed itself to be the most suited for describing the atomic Rydberg states of heavy rare gases, as pointed out before.[12,18–20] For nonpenetrating highly excited states (large l and n values) the valence electron fine structure and the exchange electrostatic interaction can be neglected in comparison with the direct electrostatic interaction, which is itself small with regard to the anisotropic ion core fine-structure splitting. This explains why nondiagonal matrix elements of the atomic Hamiltonian are quite negligible in this coupling scheme.

As we are interested in the problem of Stark coupling between $18f$ and quasihydrogenic $18l$ ($l\geq4$) configurations which completely fulfil the above conditions, the atomic states will be noted:

$$|18l[K]JM\rangle \text{ with } 3\leq l\leq 17 .$$

[l is the orbital angular momentum of the outer electron that is strongly coupled to the total angular momentum of the core j ($j=\frac{1}{2},\frac{3}{2}$). It produces a resultant momentum K weakly coupled to the spin $s=\frac{1}{2}$ of the outer electron giving the total atomic angular momentum J with a projection M. A prime on l will indicate a $j=\frac{1}{2}$ value of the core angular momentum.]

In the studied spectral region, i.e., ±2 cm^{-1} about the hydrogenic $n=18$ manifold position at $E_H=126\,771.19$ cm^{-1}, there is only one perturbing state labeled $18d[3/2]_1$ at $126\,770.5(2)$ cm^{-1}, as already mentioned in Sec. III. The other $J=1$ odd-parity states as well as all the even-parity ones are known to lie far outside this energy range.[17,1] On the other hand, a graphic multichannel quantum-defect theory (MQDT) analysis using Lu-Fano plots[21] shows that the situation is the same for the $J\neq1$ odd-parity states. Therefore it is reasonable to neglect the influence of other perturbers.

Because of strong configuration interaction the so-called $18d[3/2]_1$ level should better be described as a linear combination of the states $18d[3/2]_1$, $18d[1/2]_1$, $8d'[3/2]_1$, $20s[3/2]_1$, and $10s'[1/2]_1$ having the same parity and J value.[17] The perturber can then be written as

$$\begin{aligned}|\psi d,M\rangle=&\alpha_1|18d[3/2]_1M\rangle+\alpha_2|18d[1/2]_1M\rangle\\&+\alpha_3|8d'[3/2]_1M\rangle+\alpha_4|20s[3/2]_1M\rangle\\&+\alpha_5|10s'[1/2]_1M\rangle .\end{aligned}\tag{1}$$

A MQDT analysis of $J=1$ odd series of argon performed by Lee and Lu[22] allows us to calculate the weights of the d-state decomposition of the MQDT channels $d[3/2]_1$, $d[1/2]_1$, $d'[3/2]_1$, $s[3/2]_1$, and $s'[1/2]_1$. These weights can be taken to estimate the corresponding α_i coefficients in expansion (1).

Under this assumption we find

$$\alpha_1=0.54,\quad \alpha_2=0.76,\quad \alpha_3=0.34,\quad \alpha_4\simeq\alpha_5\simeq0 .$$

So the truncated basis will finally comprise the $|18l[K]JM\rangle$ states ($l\geq3$) together with the $|\psi d,M\rangle$ perturber substates.

We have then to estimate the zero-field energies of the basis states. The d-state perturber energy will be taken as an adjustable parameter in the vicinity of the value given by Yoshino.[17] For all the other states we assume the validity of jK coupling. Using the same method as Kelleher and Saloman,[7] energies are calculated through the diagonal contribution of the direct electrostatic interaction, stating that the relativistic fine structure of the outer electron and the exchange interaction can be neglected for these nonpenetrating Rydberg states. The zero-field energies are given in atomic units by

$$\langle 18l[K]JM|H_0|18l[K]JM\rangle=E(18l)+\Delta E(18l,K,j=\tfrac{3}{2}),$$

with

$$\Delta E=-\frac{6h^2+3h-2j(j+1)l(l+1)}{4j(j+1)(2l-1)(2l+3)}\langle r_c^2\rangle\langle r^{-3}\rangle$$

and

$$h=\tfrac{1}{2}[K(K+1)-j(j+1)-l(l+1)] .$$

$E(18l)$ is the mean energy of the $18l$ multiplicity, $\langle r_c^2\rangle$ is the mean-square radius of the core, and the mean value $\langle r^{-3}\rangle$ is relevant to the Rydberg electron and can be approximated by the hydrogenic formula.[23] ΔE describes the fine-structure splittings about the mean energy. For $l=3$, $E(18f)$ and $\langle r_c^2\rangle$ are calculated using the available experimental values of $18f[3/2]_{1,2}$ and $18f[5/2]_{2,3}$ energies (see Sec. III). For $l\geq 4$, we take $\langle r_c^2\rangle=\langle r_{\mathrm{Ar}^+}^2\rangle=2.856$ a.u. (Ref. 24), assuming these orbitals are nonpenetrating. But the nonzero values of $E(18f)-E_H$ and $\langle r_c^2\rangle_{18f}-\langle r_{\mathrm{Ar}^+}^2\rangle$ indicate that polarizability and core penetration effects should not be totally ignored for higher l values. For this reason we introduce a weak quantum defect δ_g for the $18g$ configuration. According to the only measured $5g$ configuration[25] and assuming δ_g to be independent of n, we choose $\delta_g=0.002$. For higher l states the quantum defects are set to zero.

The calculation of the off-diagonal matrix elements of the Stark Hamiltonian H_{Stark} is straightforward, making the assumption that the radial part of nonpenetrating orbitals is purely hydrogenic

$$\langle 18l[K]JM|-Fz|18l'[K']J'M'\rangle=-F(-)^{J-M+J'-1+l-l'+l_>}l_>^{1/2}(2J+1)^{1/2}(2J'+1)^{1/2}(2K'+1)^{1/2}(2K+1)^{1/2}$$
$$\times\delta_{jj'}\delta_{MM'}\begin{pmatrix} J & 1 & J' \\ -M & 0 & M'\end{pmatrix}\begin{Bmatrix}1/2 & J & K\\ 1 & K' & J'\end{Bmatrix}\begin{Bmatrix}j & 1 & K\\ 1 & K' & l'\end{Bmatrix}\langle 18l|r|18l'\rangle ,$$

where $l_>=\max(l,l')$. The quantization axis is chosen to be parallel to the static electric field direction. The selection rules are the following: $\Delta l=\pm 1$, $\Delta K=0,\pm 1$ ($K=0\not\to K'=0$), $\Delta J=0,\pm 1$ ($J=0\not\to J'=0$), $\Delta j=0$, and $\Delta M=0$. The radial matrix element is given by the hydrogenic formula

$$\langle nl|r|nl-1\rangle=\tfrac{3}{2}n(n^2-l^2)^{1/2}(\text{a.u.}) .$$

Although f is a weak penetrating orbital, the Coulomb approximation is nevertheless valid to calculate $\langle 18f|r|18g\rangle$. This is not necessarily the case for $\langle 18d|r|18f\rangle$ because the d orbital is obviously a very penetrating one, as shown by configuration mixing. This value may be different from the pure hydrogenic case. For this reason, we will take it as

$$\langle 18d|r|18f\rangle=C\langle 18d|r|18f\rangle_H,$$

C being an adjustable parameter.

The total Hamiltonian diagonalization for each M and F values gives the energies of the Stark states and their weights on the truncated basis. Owing to the selection rules in jK coupling for the electric dipole transition in the particular case of a π excitation, it is possible to calculate the relative intensities of the lines, keeping in mind that only the $3d[3/2]_2$ component of the metastable level is active in our problem: the Stark states will be connected to the lower level, and thus populated, only through their components on the $|18f[K]JM\rangle$ zero-field states.

The radial matrix element $\langle 3d|r|18f\rangle$ present in all the oscillator strengths can be eliminated, and standard angular momentum algebra provides the relative intensities in a quite reliable way if we assume that the metastable sublevels $|3d[3/2]2M\rangle$ are equipopulated and unperturbed by the electric field for weak F values.

To reproduce the Doppler broadening, the calculated lines are convoluted with a Gaussian line shape 5×10^{-3} cm^{-1} wide. To take into account a weak static field inhomogeneity, a second broadening proportional to the energy shift from the center of the $n=18$ manifold is added.

C. Theoretical results

The synthetic spectra are displayed in Fig. 4 and can be compared with the experimental map (see Fig. 1). There are a few deficiencies in the latter: the relative intensities for $F=25$ V/cm are not very reliable, the $F=85$ V/cm is not complete and the length of the scans toward the lower energies is slightly insufficient.

In spite of these blanks, agreement between theory and experiment is quite satisfactory, especially for fields higher than 40 V/cm for which the exact zero-field energy values are less critical [Fig. 2(b)]. The calculated spectra in Fig. 4 have been obtained for a d-state energy $Ed=126\,770.39$ cm^{-1} and a C-parameter close to 1, which bears out the Coulomb approximation. Not taking into account the perturber and the δ_g quantum defect makes it impossible to reproduce the more striking characteristics of low-field spectra and clearly modifies the rest of the map.

The simple model used in this study reproduces the main features of the experimental spectra. We clearly observe the birth of the $18l(l>4)$ quasihydrogenic manifold whose components become visible through their Stark mixing with the $18f$ multiplicity and exhibit a linear behavior with the electric field, as expected for near zero quantum-defect levels. On the left of the map, the large number of lines originating from the $18f$ configuration and repelled by the rest of the manifold tend to form well-defined groups as F increases. For the highest electric fields, the corresponding structures have a very similar shape along a given branch of the Stark manifold. As an example, the structure of the central region is displayed enlarged in Fig. 3(b). The appearance of 15 distinct and equidistant groups of lines for high F values

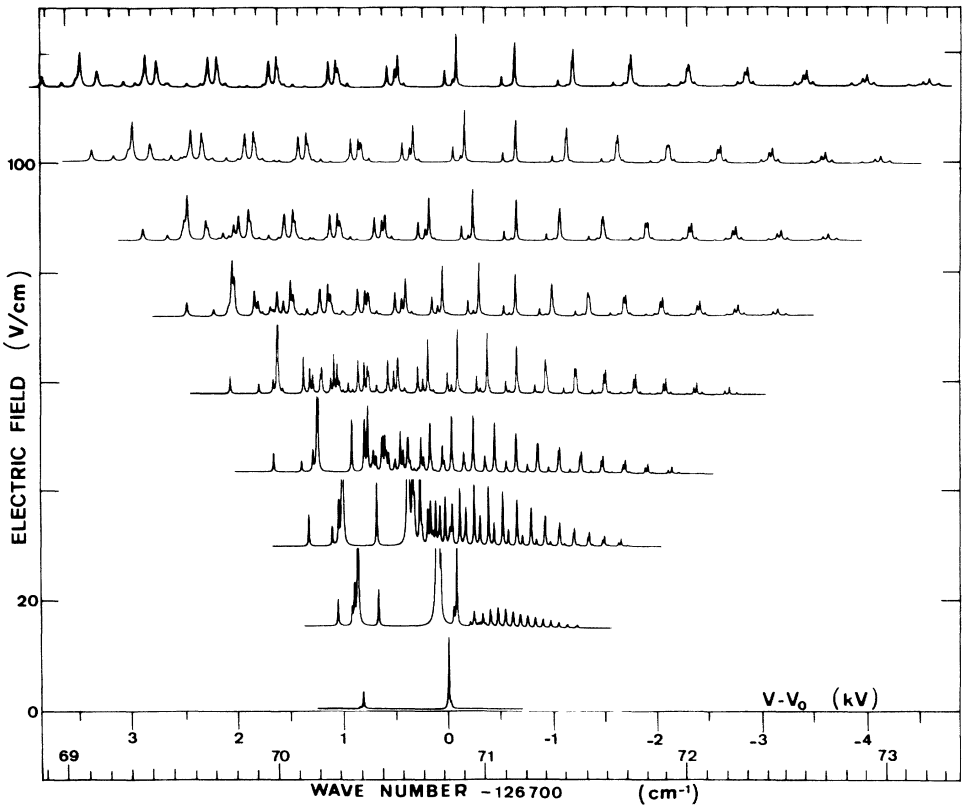

FIG. 4. Theoretical Stark map for $|M|=0,1,2$ states of argon near $n=18$. The absolute scale for line intensities is arbitrary chosen for each electric field value. Some lines may be truncated.

seems to indicate that the $18f$ components are completely merged into the rest of the manifold: in this case the electrostatic fine structure could be considered as a perturbation on the incomplete alkali-metal-like Stark pattern.[6] This fact is qualitatively confirmed in the particular case where the fine structure of argon states is neglected in a first approximation. Such a Stark map near $n=18$ is displayed in Fig. 5. The nonzero δ_g and δ_f quantum defects give rise to a typical alkali-metal-like Stark manifold which roughly represents the evolution of the fine-structure centers of gravity. One clearly observes that the mixing of $18f$ with the hydrogenic manifold occurs between 20 and 40 V/cm and is complete for fields higher than 50 V/cm. Although fine structure is too large compared with Stark splitting to be omitted, especially for $18f$ at low fields, the former remark can explain the sudden collapse of $18f[5/2]$ lines between 30 and 40 V/cm and the strong similarity between experimental spectra above 60 V/cm. Because of their complexity, the experimental spectra cannot be linked to simple physical ideas based on a perturbative approach of the problem, but they prove the validity of the theoretical model which can reliably be used for more accurate investigations.

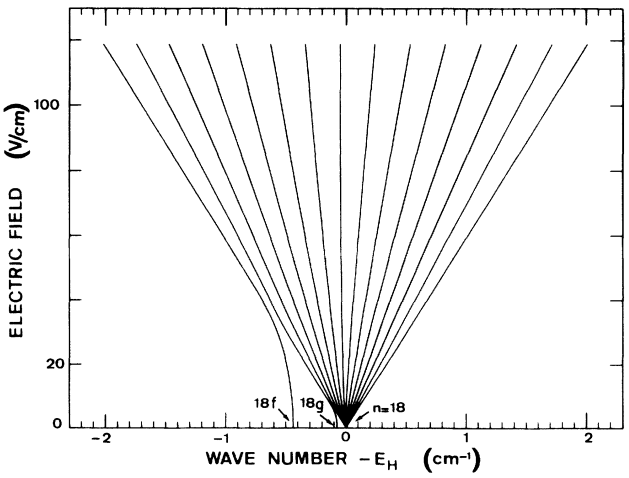

FIG. 5. Calculated Stark map near $n=18$ neglecting fine structure ($|M_l|=3$). (The zero-field position of the $18f$ and $18g$ levels and the $n=18$ hydrogenic manifold are indicated by arrows. E_H is the $n=18$ manifold energy.)

V. CONCLUSIONS

In conclusion, this study shows how the coupling of the Rydberg electron with an anisotropic ionic core generates many fine-structure sublevels from each Stark component. The jK coupling scheme proved to be fully adapted to the physical problem: it allowed us to develop a simple theoretical calculation which accurately reproduced the complex Stark spectra experimentally observed. The agreement between the predictions of the model and the experimental data is quite good not only

for the energies of the lines but also for their relative intensities.

The high resolution achieved with the collinear spectroscopy technique was essential for this experiment owing to the complexity of the structures and the great number of components close to each other. Starting from the $4s'[1/2]_0$ metastable state instead of $4s[3/2]_2$ would enable us to discriminate between $M=0$ and $|M|=1$ Stark states owing to the choice of the laser polarization. This would give rise to simpler spectra and easier interpretation. Finally the effects on the Stark spectra due to the presence of the perturber state $18d[3/2]_1$ in the studied energy range are quantitatively reproduced with our model by finally adjusting only one parameter: the exact energy of this state.

ACKNOWLEDGMENTS

We gratefully acknowledge several useful discussions concerning the theoretical treatment with Eliane Luc-Koenig from Laboratoire Aimé Cotton at Orsay. Laboratoire de Spectrométrie Ionique et Moléculaire is Unité Associée No. 171 of Centre National de la Recherche Scientifique.

[1]M. Pellarin, J. L. Vialle, M. Carré, J. Lermé, and M. Aymar, J. Phys. B **21**, 3833 (1988).
[2]M. G. Littman, M. L. Zimmerman, T. W. Ducas, R. R. Freeman, and D. Kleppner, Phys. Rev. Lett. **36**, 788 (1976).
[3]M. G. Littman, M. M. Kash, and D. Kleppner, Phys. Rev. Lett. **41**, 103 (1978).
[4]T. F. Gallagher, L. M. Humphrey, W. E. Cooke, R. M. Hill, and S. A. Edelstein, Phys. Rev. A **16**, 1098 (1977).
[5]M. L. Zimmerman, T. W. Ducas, M. G. Littman, and D. Kleppner, J. Phys. B **11**, L11 (1978).
[6]M. L. Zimmerman, M. G. Littman, M. M. Kash, and D. Kleppner, Phys. Rev. A **20**, 2251 (1979).
[7]D. E. Kelleher and E. B. Saloman, Phys. Rev. A **35**, 3327 (1987).
[8]C. Delsart and J. C. Keller, Phys. Rev. A **28**, 845 (1983).
[9]W. E. Ernst, T. P. Softley, and R. N. Zare, Phys. Rev. A **37**, 4172 (1988).
[10]R. D. Knight and L. Wang, Phys. Rev. A **32**, 896 (1985).
[11]H. Jäger and L. Windholz, Phys. Scr. **29**, 344 (1984).
[12]R. Ziegelbecker and B. Schnizer, Z. Phys. D **6**, 327 (1987).
[13]M. Aymar, Physica **57**, 178 (1971).
[14]M. Bacal, A. Truc, H. J. Doucet, H. Lamain, and M. Chrétien, Nucl. Instrum. Methods **114**, 407 (1974).
[15]Tran-Ba-Chu, A. J. Bouvier, A. Bouvier, and M. Broyer, J. Phys. (Paris) **46**, 551 (1985).
[16]S. L. Kaufman, Opt. Commun. **17**, 309 (1976).
[17]K. Yoshino, J. Opt. Soc. Am. **60** 1220 (1970).
[18]G. Racah, Phys. Rev. **61**, 537 (1942).
[19]R. D. Rundel, F. B. Dunning, H. C. Goldwire, Jr., and R. F. Stebbings, J. Opt. Soc. Am. **65**, 628 (1975).
[20]M. Aymar, O. Robaux, and C. Thomas, J. Phys. B **14**, 4255 (1981).
[21]K. T. Lu and U. Fano, Phys. Rev. A **2**, 81 (1970).
[22]C. M. Lee and K. T. Lu, Phys. Rev. A **8**, 1241 (1973).
[23]H. A. Bethe and E. E. Salpeter, *Quantum Mechanics of One-and-Two Electron Atoms* (Academic, New York, 1957).
[24]E. Luc-Koenig (private communication).
[25]C. E. Moore, *Atomic Energy Levels,* Natl. Bur. Stand. (U.S.) Circ. No. 467 (U.S. GPO, Washington, D.C., 1958), Vol. 1.